High Order On Surface Radiation Boundary Conditions For Radar Cross-Section Application

Adel Al Weshah [1] and S. I. Hariharan [2]

[1]School of Electrical and Computer Engineering
University of Georgia, Athens, GA 30602 USA
adel.alweshah@uga.edu

[2]Department of Electrical and Computer Engineering
The University of Akron, Akron, OH 44325 USA

Abstract – Solving problems governed by two and three-dimensional wave equations in exterior domains are a complex task. There are techniques to reduce the computational complexities, one such technique is On-Surface Radiation Boundary Conditions (OSRBC). There have been recent interests in revisiting this technique for two and three-dimensional problems [1]. In this paper, we explore the implementation of a new high order OSRBC based on the high order local boundary conditions introduced by [2] for two and three dimensions to solve the wave equation in unbounded domains. In most cases, it is difficult to construct exact solutions. For comparisons of numerical solutions, we use solutions obtained from large domains as approximate exact solutions. The implementation involves a two step novel approach to handle time derivatives. First, the governing equations and boundary conditions are converted to Laplace transform domain. Then, based on bilinear transformation the procedure was converted to z domain which simplified the implementation process. In particular, this process leads to higher accuracy compared to the different types of finite difference schemes used to approximate the first and second order partial derivative in the new high order OSRBC and the auxiliary functions that define the high order boundary conditions. A series of numerical tests demonstrate the accuracy and efficiency of the new high order OSRBC for two and three-dimensional problems. Both the long domain solutions as well as the new OSRBC solutions are compared for accuracies and useful results for radar cross-section calculations are presented.

Index Terms – On surface radiation boundary conditions, scattering problems, time-domain analysis, numerical analysis, bilinear transformation, radar-cross section, two and three-dimensional.

I. INTRODUCTION

Computational electromagnetics is a vast area of research and has gained a considerable amount of attention during the last four decades. This fact is due to new technological requirements and scientific applications such as electromagnetic waves scattered around an antenna and radar cross section calculations [3, 4]. This field yields yet challenging questions that require the development of efficient and accurate computational techniques for the simulation of electromagnetic scattering problems. Several computational difficulties limit the application of classical numerical approaches. The first obstacle is related to the open domain where many wave propagation problems are described in the unbounded domain. This makes it difficult to extend the computational domain to the far field due to the dissipative and dispersive nature of the direct numerical method. The other important obstacle is that the relevant calculations depend on the accuracy of the radiation boundary conditions (RBCS) and are linked to the fact that the wavelength of the incident field is smaller than the characteristic size of the scatterer [5].

The past two decades have seen many attempts to create accurate radiation boundary condition formulations to simulate scattering from two and three-dimensional obstacles. Examples are the Perfectly Matched Layer (PML) [6–8], integral equation formulations [9, 10] and the infinite element method [6, 11]. However, the computational effort needed for these methods limits their application range even if it provides some valuable results. Besides, these procedures are limited to frequency domain problems. Furthermore, PML and infinite element method cannot be used as the on surface boundary conditions because they have to be placed far away from the surface of the scatterer, and we need to derive an expression for a normal derivative on the surface of the scatterer.

An alternative approach is the On-Surface Radiation Boundary Condition (OSRBC) which is considered as the frontier between classical methods and asymptotic techniques [5]. It was introduced in the middle of the

Submitted On: May 23, 2019
Accepted On: December 15, 2019

eighties by [12, 13]. It is an approximate technique that applies local artificial boundary conditions [14–16] directly on the surface of the scatterer to determine the normal derivative. In these papers, the authors also introduce the basic method to compute the electromagnetic scattered filed from a two dimensional infinite cylinder. This method leads to the numerical solution of a set of partial differential equations set over the surface of the scatterer Γ (or on contour for a 2-D object). Specifically, this principle involves the calculation of normal derivatives on Γ. Unfortunately, the closer one brings the radiation boundary to the scatterer, the more precise the radiation condition should be. In [12, 13] the authors used either the first or second order radiation conditions. Again their work was limited to frequency domain problems namely, those of high frequencies. In this work, we present an arbitrary order OSRBC in the time domain in both two and three dimensions. The work presented here can be reduced to frequency domain analysis for time-harmonic incident fields.

In a sequence of works developed by [2] and [17], the authors consider arbitrary order boundary conditions for wave equations that use only a local operator on the boundary. In these works, they removed the use of higher order spatial normal derivatives found in the work of Bayliss and Turkel's boundary conditions [14]. In particular, the work found in [2] replaces the difficulties using only higher order time derivatives which are easier to implement. The work presented in this paper uses these results to formulate a new high order on-surface radiation boundary conditions. This forms the basis for the implementation of OSRBC in both two and three dimensions. In essence, we start with the introduction of two and three-dimensional Dirichlet problems governed by wave equations in the exterior domain. Then, we describe the long domain problems in both two and three dimensions. This yields the required normal derivative expressions ($\frac{\partial u}{\partial n}$) in both dimensions. To avoid differences in time, we consider the high order OSRBC in the $s-$domain using the Laplace transform. Then, we apply a new approach to discretize the high order OSRBC using the bilinear transformation method to implement a mapping from the $s-$domain to the $z-$domain. This eliminates choosing different types of finite difference implementations in time. We show the effectiveness of this approach vs time differencing in the numerical implementation section. Next, we apply the inverse $z-$transform and solve the high order OSRBC numerically in the form of a recursively defined sequence of equations. Finally, we verify our proposed results using numerical solutions.

II. PROBLEM DESCRIPTION

To describe the wave propagation problem, we assume that there is a TM wave incident on the bounded

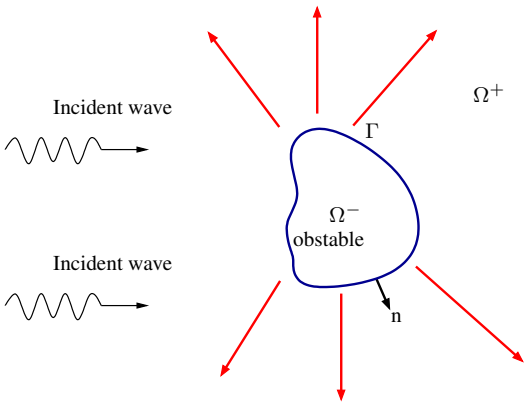

Fig. 1. Scattering Problem Configuration.

domain of $R^N (N = 2, 3)$ which represents a perfectly conducting scatterer bounded by a boundary Γ as shown in Fig. 1. We assume this domain is sufficiently smooth and **n** is the unit normal vector to Ω^-. We consider an incident TM wave field (E) illuminating the obstacle. This only has one scalar component that we denote $u(\underline{x}, t)$:

$$E_{inc} = u_{inc}(\underline{x}, t), \quad E_s = u_s(\underline{x}, t),$$

Where $\underline{x} = (x_1, ..., x_N)$ a point of R^N, $u_{inc}(\underline{x}, t)$ denotes the incident field and $u_s(\underline{x}, t)$ denotes the scattered field. This source generates a scattered field (u_s) to the obstacle (Ω^-) which satisfies the so called wave equation:

$$\nabla^2 u_s - \frac{1}{c^2}\frac{\partial^2 u_s}{\partial t^2} = 0 \qquad \text{in } \Omega^+, \tag{1}$$

For the well-posedness of the problem, the field $u_s(\underline{x}, t)$ must also satisfy a boundary condition at the surface (Γ) of the body as well as the Sommerfeld radiation condition at infinity:

$$\lim_{|\underline{x}|\to\infty} |\underline{x}|^{\frac{(N-1)}{2}} \left(\nabla u_s \cdot \frac{\underline{x}}{|\underline{x}|} + \frac{\partial u_s}{\partial t} \right) = 0,$$

Because the equation (1) is of order two, we need two boundary conditions - one on the boundary of the scatterer, and the Sommerfeld radiation condition. The first boundary condition is the Dirichlet (perfect conductor) boundary condition. Here, the scatterer is assumed to be perfectly conducting on the surface Γ (or on contour for a $2-D$ object), so the field satisfies:

$$u_s(\underline{x}, t) = -u_{inc}(\underline{x}, t) \qquad \text{on } \Gamma,$$

A second condition is an implementable approximation of the Sommerfeld radiation condition. The authors of [2] derived higher order local version of Sommerfeld boundary conditions that are both asymptotically exact and easy to implement. The derivation of this boundary condition procedure originates from the [14] whose applications are typically restricted to the first order and second order formulations due to the fact that the higher order normal derivatives are difficult to implement numerically. In contrast, the work found in [2] overcomes

this difficulty by a new formulation that involves only a single order normal derivative and which is coupled with a sequence of first differential equations in time via the use of auxiliary variables. The higher order local boundary conditions are expressed in the polar coordinates form for the two-dimensional problems and spherical coordinates for the three-dimensional problems as follows:

The high order local boundary conditions for two-dimensional case are:

$$\frac{1}{c}\frac{\partial u_s}{\partial t}+\frac{\partial u_s}{\partial r}+\frac{1}{2r}u_s=w_1, \tag{2}$$

$$\frac{1}{c}\frac{\partial \omega_j}{\partial t}+\frac{j}{r}\omega_j=\frac{(j-\frac{1}{2})^2}{4r^2}\omega_{j-1}+\frac{1}{4r^2}\frac{\partial^2\omega_{j-1}}{\partial\theta^2}+\omega_{j+1}, \quad j=1,2,... \tag{3}$$

The high order local boundary conditions for three-dimensional case are:

$$\frac{1}{c}\frac{\partial u_s}{\partial t}+\frac{\partial u_s}{\partial r}+\frac{1}{r}u_s=w_1, \tag{4}$$

$$\frac{1}{c}\frac{\partial \omega_j}{\partial t}+\frac{j}{r}\omega_j=\frac{1}{4r^2}(\bigtriangledown_s^2+j(j-1))\omega_{j-1}+\omega_{j+1}, \quad j=2,3,... \tag{5}$$

Where the spherical Laplacian given by:

$$\bigtriangledown_s^2\omega_{j-1}=\frac{1}{\sin\theta}\frac{\partial}{\partial\theta}(\sin\theta\frac{\partial\omega_{j-1}}{\partial\theta})+\frac{1}{\sin^2\theta}\frac{\partial^2\omega_{j-1}}{\partial\phi^2},$$

and ω_j's are auxiliary functions defined recursively and known as remainders, we have set:

$$\omega_0=2u_s.$$

An interesting observation here is that when we set $\omega_1=0$ the condition reduces to the well known Bayliss and Turkel condition. By a direct computation, it has been proven in [2] that:

$$\omega_j=O(r^{-2j+\frac{1}{2}}) \quad \text{for } 2-D,$$
$$\omega_j=O(r^{-2j-1}) \quad \text{for } 3-D,$$

The equations (3) and (5) can be solved to find ω_1 in terms of u_s. Using reminders of order (p) and set the order ($p+1$) to be as follows:

$$\forall j>p,\ \omega_j=0.$$

Equations (2), (3) (two-dimensional case) and (4), (5) (three-dimensional case) are designed to be implemented at a far field boundary that encloses the scatterer. They can be solved to find the radial derivative $\frac{\partial u}{\partial r}$, which represents the normal derivative $\frac{\partial u}{\partial n}$ at the surface of the far field boundary. The principle of the OSRBC is that one brings the far field boundary to coincide with the boundary of the scatterer itself. The remainder of the paper analyses the impact of this process bringing the far field conditions directly on the scatterer.

III. NUMERICAL IMPLEMENTATION

In this paper, we solve the higher order local boundary conditions in two and three dimensions to find the normal derivatives on the surface of the scatterers. A new novel numerical approach to handle the time derivative is introduced. Typically, the time derivatives approximated with finite differences. Thus, for the stability and accuracy, one must be careful how these differences are handled. They can yield implicit or explicit schemes based on the differencing used to discretize the equations (2), (3) (two-dimensional case) and (4), (5) (three-dimensional case). Now, this leads to our new approach. First, these sets of boundary conditions are transformed into Laplace transform domain because of the linearity. The Laplace transform domain problem is converted to $z-$ transform based on the bilinear transformation [18]. The bilinear transformation preserves the stability and causality when mapping a continuous time equation to discrete time. This avoids the uncertainty involving choices of time derivative difference approximations. We start by implementing the Laplace transform for the higher order local boundary conditions. Assuming the boundary Γ is a perfect conductor, $c=1$ and cylindrical mode:

$$\frac{\partial^2\omega_{j-1}}{\partial\theta^2}=-m^2 \qquad \text{for } 2-D,$$

Likewise, for spherical modes we obtain:

$$\bigtriangledown_s^2\omega_{j-1}=-m(m+1) \qquad \text{for } 3-D,$$

So, the Laplace transform for (2) and (3) are given below:

$$\frac{\partial\hat{u}}{\partial r}+(s+\frac{1}{2r})\hat{u}=\hat{w}_1, \tag{6}$$

$$(s+\frac{j}{r})\hat{\omega}_j=\frac{(j-\frac{1}{2})^2-m^2}{4r^2}\hat{\omega}_{j-1}+\hat{\omega}_{j+1}, \quad j=1,2,.... \tag{7}$$

and the Laplace transform for (4) and (5) are given below:

$$\frac{\partial\hat{u}}{\partial r}+(s+\frac{1}{r})\hat{u}=\hat{w}_1, \tag{8}$$

$$(s+\frac{j}{r})\hat{\omega}_j=\frac{j(j-1)-(m^2+m)}{4r^2}\hat{\omega}_{j-1}+\hat{\omega}_{j+1}, \quad j=1,2,3,.... \tag{9}$$

Then, we implement the mapping from the $s-$domain to the $z-$domain via bilinear transform $s=\frac{2}{T}\frac{1-z^{-1}}{1+z^{-1}}$, in the equations (6) and (7) as given below, for convenience T is taken as 1:

$$\frac{\partial\hat{u}}{\partial r}+(2\frac{1-z^{-1}}{1+z^{-1}}+\frac{1}{2r})\hat{u}=\hat{w}_1, \tag{10}$$

$$(2\frac{1-z^{-1}}{1+z^{-1}}+\frac{j}{r})\hat{\omega}_j=\frac{(j-\frac{1}{2})^2-m^2}{4r^2}\hat{\omega}_{j-1}+\hat{\omega}_{j+1}, \quad j=1,2,... \tag{11}$$

and for (8) and (9) are given below:

$$\frac{\partial \hat{u}}{\partial r} + (2\frac{1-z^{-1}}{1+z^{-1}} + \frac{1}{r})\hat{u} = \hat{w}_1, \tag{12}$$

$$(2\frac{1-z^{-1}}{1+z^{-1}} + \frac{j}{r})\hat{\omega}_j = \frac{j(j-1)-(m^2+m)}{4r^2}\hat{\omega}_{j-1} + \hat{\omega}_{j+1}, \quad j = 1, 2, 3, ... \tag{13}$$

Finally, in order to solve for the normal derivative in time domain we apply the inverse $z-$transform to the equations (10) and (11) as given below:

$$\frac{\partial \bar{u}(n,r)}{\partial r} + \frac{\partial \bar{u}(n-1,r)}{\partial r} + 2[\bar{u}(n,r) - \bar{u}(n-1,r)] + \frac{[\bar{u}(n,r) + \bar{u}(n-1,r)]}{2r} = \bar{\omega}_1(n,r) + \bar{\omega}_1(n-1,r)', \tag{14}$$

$$2(\bar{\omega}_j(n,r) - \bar{\omega}_j(n-1,r)) + \frac{j}{r}(\bar{\omega}_j(n,r) + \bar{\omega}_j(n-1,r)) = \frac{(j-\frac{1}{2})^2 - m^2}{4r^2}(\bar{\omega}_{j-1}(n,r) + \bar{\omega}_{j-1}(n-1,r)) + (\bar{\omega}_{j+1}(n,r) + \bar{\omega}_{j+1}(n-1,r)), \quad j = 1, 2, ... \tag{15}$$

and for (12) and (13) are given below:

$$\frac{\partial \bar{u}(n,r)}{\partial r} + \frac{\partial \bar{u}(n-1,r)}{\partial r} + 2[\bar{u}(n,r) - \bar{u}(n-1,r)] + \frac{[\bar{u}(n,r) + \bar{u}(n-1,r)]}{r}) = \bar{\omega}_1(n,r) + \bar{\omega}_1(n-1,r), \tag{16}$$

$$2(\bar{\omega}_j(n,r) - \bar{\omega}_j(n-1,r)) + \frac{j}{r}(\bar{\omega}_j(n,r) + \bar{\omega}_j(n-1,r)) = \frac{j(j-1)-(m^2+m)}{4r^2}(\bar{\omega}_{j-1}(n,r) + \bar{\omega}_{j-1}(n-1,r)) + (\bar{\omega}_{j+1}(n,r) + \bar{\omega}_{j+1}(n-1,r)), \quad j = 1, 2, 3, ... \tag{17}$$

Solving (15) numerically to find ω_j's remainders, one needs to write these equations in the matrix form as below [19], [20]:

$$A_j\bar{\omega}^{j-1} = T_j\bar{\omega}^j - B\bar{\omega}^{j+1}, \tag{18}$$

Where A_j, T_j and B are $N \times N$ matrices given by:

$$A_j = \begin{pmatrix} a_j & 0 & 0 & \dots & 0 \\ a_j & a_j & 0 & \ddots & \vdots \\ 0 & a_j & \ddots & \ddots & 0 \\ \vdots & \ddots & \ddots & \ddots & 0 \\ 0 & \dots & 0 & a_j & a_j \end{pmatrix}$$

$$T_j = \begin{pmatrix} c_j & 0 & \dots & \dots & 0 \\ b_j & c_j & \ddots & & \vdots \\ \vdots & \ddots & \ddots & \ddots & \vdots \\ \vdots & & \ddots & \ddots & 0 \\ 0 & \dots & \dots & b_j & c_j \end{pmatrix}$$

$$B = \begin{pmatrix} 1 & 0 & \dots & \dots & 0 \\ 1 & 1 & \ddots & & \vdots \\ \vdots & \ddots & \ddots & \ddots & \vdots \\ \vdots & & \ddots & \ddots & 0 \\ 0 & \dots & \dots & 1 & 1 \end{pmatrix}$$

With:

$$a_j = \frac{(j-\frac{1}{2})^2 - m^2}{4r^2},$$

$$b_j = \frac{j}{r} - 2,$$

$$c_j = 2 + \frac{j}{r},$$

We use p auxiliary function such that $\bar{\omega}^j = 0 \; \forall j > p$, so $\bar{\omega}^{p+1} = 0$. From (18) we find that:

$$\begin{cases} \bar{\omega}^{j-1} = A_j^{-1}T_j\bar{\omega}^j - A_j^{-1}B\bar{\omega}^{j+1} \\ \bar{\omega}^{p-1} = A_p^{-1}T_p\bar{\omega}^p \end{cases},$$

we can write:

$$\begin{cases} \bar{\omega}^{p-1} = P_{p-1}\bar{\omega}^p \\ \bar{\omega}^p \quad = P_p\bar{\omega}^p \end{cases}, \tag{19}$$

where:

$$P_p = I_N and P_{p-1} = A_p^{-1}T_p,$$

To prove that $\bar{\omega}^m = P_m\bar{\omega}^p$ for every $m \leqslant p$. Using (18) we can write:

$$\begin{aligned} \bar{\omega}^{m-1} &= A_m^{-1}T_m\bar{\omega}^m - A_m^{-1}B\bar{\omega}^{m+1} \\ &= A_m^{-1}T_mP_m\bar{\omega}^p - A_m^{-1}BP_{m+1}\bar{\omega}^p \\ &= \underbrace{(A_m^{-1}T_mP_m - A_m^{-1}BP_{m+1})}_{P_{m-1}}\bar{\omega}^p, \end{aligned} \tag{20}$$

where $m \in \{1, 2, \dots, p-1\}$: From(19) and (20), we can calculate the matrices P_m's numerically using the recursive definition as given below:

$$\begin{cases} P_{m-1} = A_m^{-1}(T_mP_m - BP_{m+1}) \; \forall m \in \{1; \dots; p-1\} \\ P_{p-1} = A_p^{-1}T_p \\ P_p \quad = I_N \end{cases}, \tag{21}$$

From (21) and using the fact that $\bar{\omega}^0 = 2\bar{U}$ we can show that:

$$\bar{\omega}^0 = 2\bar{U} = P_0\bar{\omega}^p \quad \Rightarrow \quad \bar{\omega}^p = 2P_0^{-1}\bar{U},$$

and

$$\bar{\omega}^1 = P_1\bar{\omega}^p = 2P_1P_0^{-1}\bar{U}, \tag{22}$$

Solving (14) numerically to find $\frac{\partial\bar{u}(n,r)}{\partial r}\Big|_{r\in\Gamma}$, , we write it in matrix form as below:

$$\bar{V} = \bar{\omega}^1 + B^{-1}C\bar{U}, \tag{23}$$

where,

$$\bar{U} = [\bar{u}(1,R), \bar{u}(2,R), \ldots, \bar{u}(N,R)]^T$$
$$\bar{V} = [\bar{v}(1,R), \bar{v}(2,R), \ldots, \bar{v}(N,R)]^T$$

and

$$\bar{v}(n,R) = \frac{\partial\bar{u}(n,r)}{\partial r}(ndt, r\in\Gamma),$$

Also,

$$C = \begin{pmatrix} a & 0 & \ldots\ldots & 0 \\ b & a & 0 & \vdots \\ \vdots & \ddots & \ddots & \ddots \\ \vdots & & \ddots & \ddots & 0 \\ 0 & \ldots\ldots & b & a \end{pmatrix} \quad \text{is an (N) } \times \text{ (N) matrix,}$$

with:

$$a{=}-(2+\tfrac{1}{2r}),$$

$$b{=}2-\tfrac{1}{2r},$$

Then using (22) in (23) :

$$\bar{V} = (2P_1P_0^{-1} + B^{-1}C)\bar{U}, \tag{24}$$

So, for the two-dimensional case calculation of P_0 and P_1 can be done using the recursive definition given in (21). Once calculated, they allow the calculation of $\bar{V}$ which represents the normal derivative in time domain $\frac{\partial\bar{u}(n,r)}{\partial r}(ndt, r\in\Gamma)$.

For the three-dimensional case we follow the same procedure as in the two dimensional. We do this by solving (16) and (17) numerically and finding the normal derivative in the time domain $\frac{\partial\bar{u}(n,r)}{\partial r}(ndt, r\in\Gamma)$ for the three dimensional case. The only difference between the three and two dimensions solution procedure is the elements of matrix A_j and C. For matrix A_j:

$$a_j{=}\tfrac{j(j-1)-(m^2+m)}{4r^2},$$

and for matrix C:

$$a{=}-(2+\tfrac{1}{r}),$$

$$b{=}2-\tfrac{1}{r},$$

To evaluate the long domain solutions for the boundary conditions in the two and three-dimensional cases and obtain the normal derivative at the boundary Γ, we assume a perfect conductor, $c = 1$, cylindrical modes for two dimensions and spherical modes for three dimensions. We start by deriving the finite difference scheme for the wave equations in two and three dimensions:

The cylindrical mode the two-dimensional equation reduces to:

$$\frac{\partial^2 u}{\partial t^2} = \frac{\partial^2 u}{\partial r^2} + \frac{1}{r}\frac{\partial u}{\partial r} - \frac{n^2}{r^2}u, \tag{25}$$

For the three-dimensional case, spherical mode equation reduces to:

$$\frac{\partial^2 u}{\partial t^2} = \frac{\partial^2 u}{\partial r^2} + \frac{2}{r}\frac{\partial u}{\partial r} - \frac{n(n+1)}{r^2}u, \tag{26}$$

By letting $u_k^p = u(r_k, t_p)$, thus equations (25) and (26) can be approximated by:

For two-dimensional:

$$\frac{\partial^2 u_k^p}{\partial t^2} = \frac{\partial^2 u_k^p}{\partial r^2} + \frac{1}{r_k}\frac{\partial u_k^p}{\partial r} - \frac{n^2}{r_k^2}u_k^p, \tag{27}$$

For three-dimensional:

$$\frac{\partial^2 u_k^p}{\partial t^2} = \frac{\partial^2 u_k^p}{\partial r^2} + \frac{2}{r_k}\frac{\partial u_k^p}{\partial r} - \frac{n(n+1)}{r_k^2}u_k^p, \tag{28}$$

The second order partial derivative can be approximated by second order central differences and the first order partial derivative can be approximated by an average central difference. Where the second order central differences and the first order partial derivatives are defined in section VI.

For two-dimensional:

$$\frac{u_k^{p+1} - 2u_k^p + u_k^{p-1}}{(dt)^2} = \frac{u_{k+1}^p - 2u_k^p + u_{k-1}^p}{(dr)^2} + \frac{1}{2r_k}\frac{u_{k+1}^p - u_{k-1}^p}{dr} - \frac{n^2}{r_k^2}u_k^p, \tag{29}$$

For three-dimensional:

$$\frac{u_k^{p+1} - 2u_k^p + u_k^{p-1}}{(dt)^2} = \frac{u_{k+1}^p - 2u_k^p + u_{k-1}^p}{(dr)^2} + \frac{1}{r_k}\frac{u_{k+1}^p - u_{k-1}^p}{dr} - \frac{n(n+1)}{r_k^2}u_k^p, \tag{30}$$

To discretize the high order local boundary conditions, an explicit finite difference approximation is derived as follows:

By letting $w_j^p = w_j(t_p)$, the two-dimensional equations (2) and (3) can be approximated by:

$$\frac{\partial u_k^p}{\partial t} + \frac{\partial u_k^p}{\partial r} + \frac{1}{2r_k}u_k^p = w_1^p, \tag{31}$$

$$\frac{\partial w_j^p}{\partial t} + \frac{j}{r_k}w_j^p = \frac{(j-\frac{1}{2})^2 - n^2}{4r_k^2}w_{j-1}^p + w_{j+1}^p, \quad j = 1, 2, \ldots \tag{32}$$

For the case of three-dimensional equations (4) and (5) can be approximated by:

$$\frac{\partial u_k^p}{\partial t} + \frac{\partial u_k^p}{\partial r} + \frac{1}{r_k}u_k^p = w_1^p, \tag{33}$$

$$\frac{\partial w_j^p}{\partial t} + \frac{j}{r_k}w_j^p = \frac{j(j-1) - (n^2+n)}{4r_k^2}w_{j-1}^p + w_{j+1}^p, \quad j = 1, 2, 3, \ldots \tag{34}$$

The radial derivative is approximated using a backward difference and average the terms with respect to time in (31) and (33) see section VI. A forward average for time and a backward average for the radius are used to approximate the third term in (31) and (33). Lastly, use a weighted average in time to approximate w_1^p:

$$w_1^p = \frac{3}{2}w_1^p - \frac{1}{2}w_1^{p-1},$$

Similarly, the time derivative in the auxiliary functions that define the higher order boundary condition (32) and (34) can be approximated using a first order forward difference, and a forward average in time to approximate w_j^p and w_{j-1}^p. The last term w_{j+1}^p approximate using a weighted average in time.

For two-dimensional problem:

$$\frac{1}{2dt}((u_k^{p+1}+u_{k-1}^{p+1})-(u_k^p+u_{k-1}^p))+\frac{1}{2dr}((u_k^{p+1}+u_k^p) - (u_{k-1}^{p+1}+u_{k-1}^p)) + \frac{1}{8R}(u_k^{p+1}+u_{k-1}^{p+1}+u_k^p+u_{k-1}^p) = \frac{3}{2}w_1^p - \frac{1}{2}w_1^{p-1}, \quad (35)$$

$$\frac{1}{dt}(w_j^{p+1}-w_j^p)+\frac{j}{2R}(w_j^{p+1}+w_j^p) = \frac{(j-\frac{1}{2})^2-n^2}{8R^2}(w_{j-1}^{p+1}+w_{j-1}^p)+\frac{3}{2}w_{j+1}^p-\frac{1}{2}w_{j+1}^{p-1}, \quad (36)$$

For the three-dimensional problem:

$$\frac{1}{2dt}((u_k^{p+1}+u_{k-1}^{p+1})-(u_k^p+u_{k-1}^p))+\frac{1}{2dr}((u_k^{p+1}+u_k^p) - (u_{k-1}^{p+1}+u_{k-1}^p)) + \frac{1}{4R}(u_k^{p+1}+u_{k-1}^{p+1}+u_k^p+u_{k-1}^p) = \frac{3}{2}w_1^p - \frac{1}{2}w_1^{p-1}, \quad (37)$$

$$\frac{1}{dt}(w_j^{p+1}-w_j^p)+\frac{j}{R}(w_j^{p+1}+w_j^p) = \frac{j(j-1)-(n^2+n)}{8R^2}(w_{j-1}^{p+1}+w_{j-1}^p)+\frac{3}{2}w_{j+1}^p-\frac{1}{2}w_{j+1}^{p-1}, \quad (38)$$

and in both cases the normal derivative ($\frac{\partial u}{\partial r}$) can be approximated using a backward difference and average the terms with respect to time as follows:

$$\frac{\partial u}{\partial r} = \frac{(u_k^{p+1}+u_k^p)-(u_{k-1}^{p+1}+u_{k-1}^p)}{2dr}, \quad (39)$$

We solve these equations sequentially. In [2] the authors prove that:

$$\omega_j = O(r^{-2j+\frac{1}{2}}) \text{ for } 2-D,$$
$$\omega_j = O(r^{-2j-1}) \text{ for } 3-D,$$

We can infer that the remainder becomes zero after fixed arbitrarily j depending on the desired accuracy. Let us call the last non-zero remainder ω_N, that is all remainder ω_j with $j > N$ is neglected and assumed to be zero. Therefore, (w_{j+1}) is smaller than (w_j) and (w_1) is smaller than (w_0). The boundary conditions are applied halfway between the last two meshes.

This procedure allows the calculation of the long domain normal derivative of the scattered field ($\frac{\partial u_s}{\partial r}$) at the surface of the scatterer. The radar cross section (RCS) of a scatterer can be solved using the on surface radiation boundary conditions. The scattered field ($U_s(\underline{x})$) at some distance from the scatterer boundary Γ is given by [12]:

$$U_s(\underline{x}) = \int_\Gamma \left[G(\underline{x},\underline{y})\frac{\partial U_s(\underline{y}))}{\partial n} - U_s(\underline{y})\frac{\partial G(\underline{x},\underline{y})}{\partial n}\right] ds, \quad (40)$$

Where $G(\underline{x},\underline{y})$ is the free space Green's function given by:

$$G(\underline{x},\underline{y}) = -(i/4)H_0^1(kd) \quad \text{for } 2-D,$$
$$G(\underline{x},\underline{y}) = \frac{e^{ikd}}{4\pi d} \quad \text{for } 3-D,$$

and, $d = |\underline{x}-\underline{y}|$, $\frac{\partial}{\partial n}$ is the outward normal derivative on Γ, $\underline{y}$ is on Γ, $\underline{x}$ is some distance from Γ, U_s is the Fourier transform of u_s, and k is the wave number. It is known that the far field expansion of (40) for two and three dimensional can be written as:

$$U_s(\underline{x}) = A_0\frac{e^{ikr}}{\sqrt{r}} \quad \text{for } 2-D, \quad (41)$$

$$U_s(\underline{x}) = \bar{A_0}\frac{e^{ikr}}{r} \quad \text{for } 3-D, \quad (42)$$

Where the term A_0 in (41) is given by (see section VII):

$$A_0 = \frac{e^{j\pi 4}}{\sqrt{8k\pi}}\int_\Gamma \left[\frac{\partial U_s(\underline{y})}{\partial n} - jk\cos\delta U_{inc}(\underline{y})\right] e^{-jk\psi}ds, \quad (43)$$

and $\bar{A_0}$ in (42) is given by (see section VII):

$$\bar{A_0} = \frac{1}{4\pi}\int_\Gamma \left[\frac{\partial U_s(\underline{y})}{\partial n} - jk\cos\delta U_{inc}(\underline{y})\right] e^{-jk\psi}ds, \quad (44)$$

Where $\cos\delta = \hat{\underline{x}}.\hat{n}$ and $\psi = \hat{\underline{x}}.\underline{y}$. The RCS can be calculated using A_0 by the following expression:

$$RCS = 10\log_{10}(2\pi R|A_0|^2) \quad \text{for } 2-D, \quad (45)$$
$$RCS = 10\log_{10}(4\pi R^2|\bar{A_0}|^2) \quad \text{for } 3-D, \quad (46)$$

IV. RESULTS

To demonstrate the results obtained for a circular and spherical scatterer, we developed a series of numerical tests. The first example is for the incident field on the perfectly conducting sphere of radius one for the three dimensional case (a disk of radius one for the two dimensional case).

For two dimensional:

$$u_{inc}(\underline{x},t) = \frac{1-\cos 2\pi t}{1+t^2}\cos n\theta, \quad (47)$$

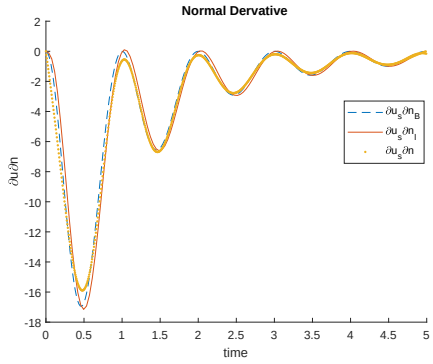

Fig. 2. Comparison of long domain ($\partial u_s \partial n_l$), the finite difference scheme for OSRBC ($\partial u_s \partial n$) and the bilinear method for OSRBC ($\partial u_s \partial n_B$) solutions for normal derivative at $t = 5$ for the two-dimensional case.

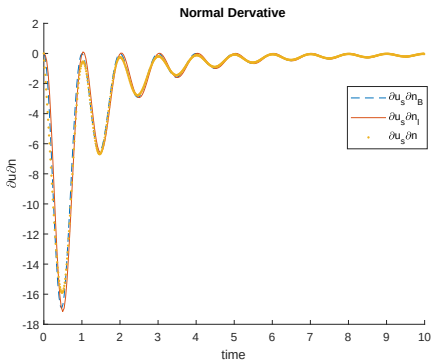

Fig. 3. Comparison of long domain ($\partial u_s \partial n_l$), the finite difference scheme for OSRBC ($\partial u_s \partial n$) and the bilinear method for OSRBC ($\partial u_s \partial n_B$) solutions for normal derivative at $t = 10$ for the two-dimensional case.

For three dimensional:

$$u_{inc}(\underline{x}, t) = \frac{1 - \cos 2\pi t}{1 + t^2}(\cos m\phi + \sin m\phi) P_n^m(\cos n\theta), \tag{48}$$

The normal derivative for the long domain solution ($\frac{\partial u_{long}}{\partial n}$) is calculated for the artificial boundary condition at the location $R = 10$. The long domain solution ($\frac{\partial u_{long}}{\partial n}$) compared with the normal derivative ($\frac{\partial u}{\partial n}$) calculated using the high order OSRBC at the surface of the scatterer. Two numerical approaches are used to discretize the high order OSRBC at the surface of the scatterer in a time domain. The first approach is the finite difference scheme. The second approach is the bilinear method. Both approaches are described in section 3. Figure 2 compares the normal derivatives (2-dimensional case) at $dr = 0.8dt$, $t = 5$, $c = 1$, the order of auxiliary functions $N = 5$, the high order boundary conditions at the surface of the scatterer with $R = 1$ and $n = 10$. Figure 3 compares the results for the same conditions but for $t = 10$ and the order of auxiliary functions $N = 8$. The figures show that discretize the high order OSRBC in the time domain using the bilinear method leads to higher accuracy compared to a finite difference scheme under the same variable values. Also, Fig. 3 clearly shows that the error decreases when t and the number of auxiliary functions N are increased. Figure 4 and Fig. 5 compare the results for the three-dimensional case. The results are almost identical to the two-dimensional case where the bilinear method gives the smallest error compare to the finite difference scheme. Clearly, the normal derivative ($\frac{\partial u}{\partial n}$) calculated using the high order OSRBC at the surface of the scatterer in the time domain gives better results for the three- dimensional case compared to the two-dimensional case. To compare the long domain solution for the normal derivative ($\partial u_{sl} \partial n$) with the high order on surface radiation boundary conditions solution

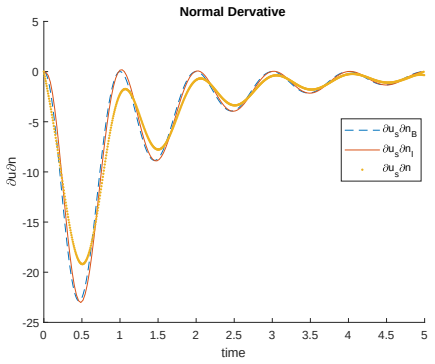

Fig. 4. Comparison of long domain ($\partial u_{sl} \partial n$), the finite difference scheme for OSRBC ($\partial u_s \partial n$) and the bilinear method for OSRBC ($\partial u_s \partial n_B$) solutions for normal derivative at $t = 5$ for the three-dimensional case.

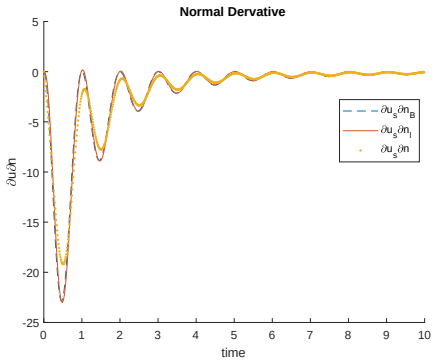

Fig. 5. Comparison of long domain ($\partial u_{sl} \partial n$), the finite difference scheme for OSRBC ($\partial u_s \partial n$) and the bilinear method for OSRBC ($\partial u_s \partial n_B$) solutions for normal derivative at $t = 10$ for the three-dimensional case.

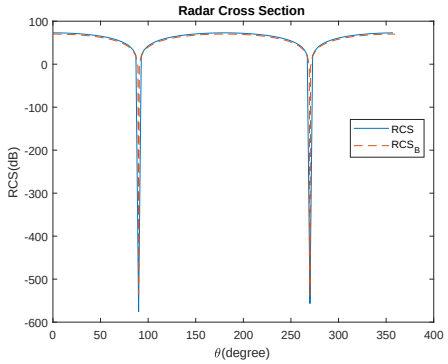

Fig. 6. Comparison of RCS calculation using the long solution and the OSRBC solution based on bilinear method for the two-dimensional case.

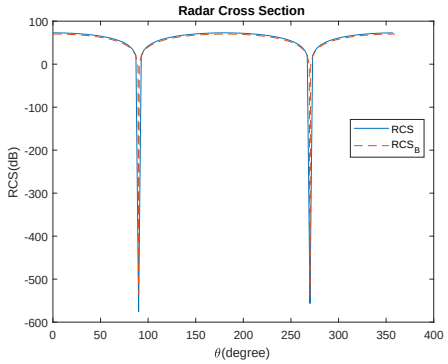

Fig. 7. Comparison of RCS calculation using the long solution and the OSRBC solution based on bilinear method for the three-dimensional case.

($\partial u_s \partial n_B$), we did numerical computations to calculate the Radar Cross Section (RCS) as defined by equations (45) and (46) and shown in Fig. 6 and Fig. 7. We observe that the results are almost identical for both solutions and calculating the RCS using the bilinear method solution for the normal derivative ($\partial u_s \partial n_B$) needed less computational time compared to the long domain solution for the normal derivative ($\partial u_{sl} \partial n$).

V. CONCLUSION

This paper presents a new high order time domain OSRBCs based on high order boundary condition introduced by [2] in two and three dimensions. The thrust of the OSRBC is to calculate the normal derivative on the scatterer. Once the normal derivative is calculated, an application to calculate radar cross sections is presented. As shown in the analysis and the numerical implementations, two different procedures have been used to calculate the normal derivative ($\partial u \partial n$). The first procedure based on the new high order OSRBC which calculates accurately and efficiently the normal derivatives ($\partial u \partial n$) on the surface of the scatterer. The second procedure is the exact solution based on long domain solutions ($\partial u_{sl} \partial n$). These two procedures are used to calculate errors. The new high order OSRBC results in a smaller error when the order of the auxiliary functions is increased. Numerical examples are provided for calculating the normal derivatives and radar cross section. Bilinear transform techniques used to discretize the new high order OSRBC and the auxiliary functions. This technique is contrasted with the traditional differencing to approximate time derivatives. The use of the bilinear transformation leads to higher accuracy and substantial simplifications in implementations when compared to the different types of standard finite difference schemes used to discretize the higher order OSRBCs and the auxiliary functions. This procedure can be extended to full Maxwell's equations and is currently under investigation.

VI. PARTIAL DERIVATIVES APPROXIMATION

It can be shown in [21] that the partial derivatives can be approximated by second order central differences as:

$$\frac{\partial^2 u_k^p}{\partial t^2} = \frac{u_k^{p+1} - 2u_k^p + u_k^{p-1}}{(dt)^2}, \tag{49}$$

$$\frac{\partial^2 u_k^p}{\partial r^2} = \frac{u_{k+1}^p - 2u_k^p + u_{k-1}^p}{(dr)^2}, \tag{50}$$

The average central differences approximation for first order partial derivative define as:

$$\frac{\partial u_k^p}{\partial r} = \frac{u_{k+1}^p - u_{k-1}^p}{2dr}, \tag{51}$$

The backward difference and average the term with respect to time is used to approximate the first order partial derivative is define as:

$$\frac{\partial u_k^p}{\partial r} = \frac{1}{2dr}((u_k^{p+1} + u_k^p) - (u_{k-1}^{p+1} + u_{k-1}^p)), \tag{52}$$

The forward average for time and a backward average for the radius is define as:

$$\frac{u_k^p}{r_k} = \frac{u_k^{p+1} + u_{k-1}^{p+1} + u_k^p + u_{k-1}^p}{4r}, \tag{53}$$

VII. RADAR CROSS SECTION CALCULATION

A. Radar cross section calculation for two-dimensional case

For the scatterer with boundary Γ, the Green's second identity is used to calculate the scattered field ($U_s(\underline{x})$) at some distance from the scatterer boundary Γ is given by [12]:

$$U_s(\underline{x}) = \int_\Gamma \left[G(\underline{x}, \underline{y}) \frac{\partial U_s(\underline{y}))}{\partial n} - U_s(\underline{y}) \frac{\partial G(\underline{x}, \underline{y})}{\partial n} \right] ds_{\underline{y}}, \tag{54}$$

Where $G(\underline{x},\underline{y})$ is the free space Green's function given by:

$$G(\underline{x},\underline{y}) = -(i/4)H_0^1(kd) \quad \text{for } 2-D, \tag{55}$$

$$G(\underline{x},\underline{y}) = \frac{e^{ikd}}{4\pi d} \quad \text{for } 3-D, \tag{56}$$

and, $d = \left|\underline{x}-\underline{y}\right|$, $\frac{\partial}{\partial n}$ is the outward normal derivative on Γ, $\underline{y}$ is on Γ, $\underline{x}$ at some distance from Γ, $U_s(\underline{x})$ is the Fourier transform of $u_s(\underline{x})$, and k is the wave number.
To evaluate the integral in (54), we need to find the $\frac{\partial G(\underline{x},\underline{y})}{\partial n}$ for two dimensions:

$$\frac{\partial G(\underline{x},\underline{y})}{\partial n} = \frac{ik}{4}H_1^1(k\left|\underline{x}-\underline{y}\right|)\frac{\partial}{\partial n}\left|\underline{x}-\underline{y}\right|, \tag{57}$$

$$\begin{aligned}\tfrac{\partial}{\partial n}\left|\underline{x}-\underline{y}\right| &= \tfrac{\partial}{\partial n}\sqrt{(x_1-y_1)^2+(x_2-y_2)^2}\\ &= \bigtriangledown(\sqrt{(x_1-y_1)^2+(x_2-y_2)^2})\cdot\hat{n_{\underline{y}}},\\ &= \tfrac{(y_1-x_1)i+(y_2-x_2)j}{\sqrt{(x_1-y_1)^2+(x_2-y_2)^2}}\cdot\hat{n_{\underline{y}}}\end{aligned} \tag{58}$$

When $\underline{x}\to\infty$ the (59) becomes:

$$\begin{aligned}\tfrac{\partial}{\partial n}\left|\underline{x}-\underline{y}\right| &= -\tfrac{(x_1)i+(x_2)j}{\sqrt{(x_1)^2+(x_2)^2}}\cdot\hat{n_{\underline{y}}}\\ &= -\hat{\underline{x}}\cdot\hat{n_{\underline{y}}}\\ &= -\cos\delta,\end{aligned} \tag{59}$$

The asymptotic approximation for the Hankel function [22] H_0^1 and H_1^1 when $d\to\infty$ is given as:

$$\frac{i}{4}H_0^1(d) = \sqrt{\frac{1}{8\pi d}}e^{i(d+\frac{\pi}{4})},$$

$$\frac{i}{4}H_1^1(d) = i\sqrt{\frac{1}{8\pi d}}e^{i(d+\frac{\pi}{4})},$$

Assume $d = k\left|\underline{x}-\underline{y}\right|$ and using the law of cosine:

$$d = k\sqrt{\left|\underline{x}\right|^2+\left|\underline{y}\right|^2-2\left|\underline{x}\right|\left|\underline{x}\right|\cos\gamma},$$

As $\underline{x}\to\infty$,

$$d \simeq k(|\underline{x}|-\left|\underline{y}\right|\cos\gamma),$$

Now, as $d\to\infty$,

$$d \simeq kr - k\psi, \tag{60}$$

Where r is the distance from the center of the scatterer to the point $\underline{x}$ and $\psi = \left|\underline{y}\right|\cos\gamma = R\cos(\theta-\theta')$. Thus, we can use the (60) in (55). Now the (54):

$$\begin{aligned}U_s(\underline{x}) &= \int_\Gamma \sqrt{\frac{1}{8\pi(kr-k\psi)}}e^{i((kr-k\psi)+\frac{\pi}{4})}\frac{\partial U_s(\underline{y}))}{\partial n}\\ &- U_s(\underline{y})ik\sqrt{\frac{1}{8\pi(kr-k\psi)}}e^{i((kr-k\psi)+\frac{\pi}{4})}\cos\delta ds_{\underline{y}} =\\ &\frac{e^{\frac{-i\pi}{4}}}{\sqrt{8\pi kr}}\int_\Gamma\left[\frac{\partial U_s(\underline{y}))}{\partial n}+ik\cos\delta U_s(\underline{y})e^{ikr}e^{-ik\psi}\right]ds_{\underline{y}},\end{aligned} \tag{61}$$

Where $U_s(\underline{y})\mid_\Gamma = -U_{inc}(\underline{y})$,

$$\begin{aligned}&U_s(\underline{x}) =\\ &\frac{e^{\frac{-i\pi}{4}}}{\sqrt{8\pi kr}}\int_\Gamma\left[\frac{\partial U_s(\underline{y}))}{\partial n}-ik\cos\delta U_{inc}(\underline{y})e^{ikr}e^{-ik\psi}\right]ds_{\underline{y}},\end{aligned} \tag{62}$$

B. Radar cross section calculation for three-dimensional case

For three-dimensional, the Green's function given by:

$$G(\underline{x},\underline{y}) = \frac{e^{ikd}}{4\pi d} \quad \text{for } 3-D, \tag{63}$$

To evaluate the integral in (54), we need to find the $\frac{\partial G(\underline{x},\underline{y})}{\partial n}$ for three dimensions:

$$\frac{\partial G(\underline{x},\underline{y})}{\partial n} = \bigtriangledown G\cdot\hat{n}, \tag{64}$$

Where:

$$\bigtriangledown G = \tfrac{e^{ikd}}{4\pi d}\left[ik-\tfrac{1}{d}\right]\left(\tfrac{(y_1-x_1)i+(y_2-x_2)j+(y_3-x_3)k}{\sqrt{(x_1-y_1)^2+(x_2-y_2)^2+(x_3-y_3)^2}}\right), \tag{65}$$

As $\underline{x}\to\infty$,

$$d \simeq k(|\underline{x}|-\left|\underline{y}\right|\cos\gamma),$$

and, as $d\to\infty$,

$$d \simeq kr - k\psi, \tag{66}$$

Thus, we can use the (66) in (64).

$$\begin{aligned}\tfrac{\partial G(\underline{x},\underline{y})}{\partial n} &= \tfrac{e^{ik(r-\psi)}}{4\pi(r-\psi)}\left[ik-\tfrac{1}{r-\psi}\right](-\cos\gamma)\\ &\simeq \tfrac{-ike^{ik(r-\psi)}}{4\pi(r-\psi)}\cos\gamma,\end{aligned} \tag{67}$$

Now, using the (67) in (54):

$$\begin{aligned}U_s(\underline{x}) &= \tfrac{e^{ikr}}{4\pi r}\int_\Gamma\left[\frac{\partial U_s(\underline{y})}{\partial n}+jk\cos\delta U_s(\underline{y})\right]e^{-jk\psi}ds_{\underline{y}}\\ &= \tfrac{e^{ikr}}{4\pi r}\int_\Gamma\left[\frac{\partial U_s(\underline{y})}{\partial n}-jk\cos\delta U_{inc}(\underline{y})\right]e^{-jk\psi}ds_{\underline{y}},\end{aligned} \tag{68}$$

Where $U_s(\underline{y})\mid_\Gamma = -U_{inc}(\underline{y})$.

REFERENCES

[1] H. Alzubaidi, X. Antoine, and C. Chniti, "Formulation and accuracy of on-surface radiation conditions for acoustic multiple scattering problems," *Applied Mathematics and Computation*, vol. 277, pp. 82–100, 2016.

[2] T. Hagstrom and S. I. Hariharan, "A formulation of asymptotic and exact boundary conditions using local operators," *Applied Numerical Mathematics*, vol. 27, no. 4, pp. 403–416, 1998.

[3] X. Antoine, "Advances in the on-surface radiation condition method: Theory, numerics and applications," *Computational Methods for Acoustics Problems*, pp. 169–194, 2008.

[4] Y. Mao, A. Z. Elsherbeni, S. Li, and T. Jiang, "Surface impedance absorbing boundary for terminating fdtd simulations." *Applied Computational Electromagnetics Society Journal*, vol. 29, no. 12, 2014.

[5] X. Antoine, M. Darbas, and Y. Y. Lu, "An improved on-surface radiation condition for acoustic scattering problems in the high-frequency spectrum," *Comptes Rendus Mathematique*, vol. 340, no. 10, pp. 769–774, 2005.

[6] L. L. Thompson, "A review of finite-element methods for time-harmonic acoustics," *The Journal of the Acoustical Society of America*, vol. 119, no. 3, pp. 1315–1330, 2006.

[7] J.-P. Berenger, "A perfectly matched layer for the absorption of electromagnetic waves," *Journal of Computational Physics*, vol. 114, no. 2, pp. 185–200, 1994.

[8] I. Mahariq, M. Kuzuoğlu, and I. Tarman, "On the attenuation of the perfectly matched layer in electromagnetic scattering problems with the spectral element method." *Applied Computational Electromagnetics Society Journal*, vol. 29, no. 9, 2014.

[9] J.-C. Nédélec, *Acoustic and Electromagnetic Equations: Integral Representations for Harmonic Problems*. Springer Science & Business Media, 2001, vol. 144.

[10] D. Colton and R. Kress, *Integral Equation Methods in Scattering Theory*. SIAM, 2013, vol. 72.

[11] F. Ihlenburg, *Finite Element Analysis of Acoustic Scattering*. Springer Science & Business Media, 2006, vol. 132.

[12] G. Kriegsmann, A. Taflove, and K. Umashankar, "A new formulation of electromagnetic wave scattering using an on-surface radiation boundary condition approach," *IEEE Transactions on Antennas and Propagation*, vol. 35, no. 2, pp. 153–161, 1987.

[13] G. A. Kriegsmann and T. Moore, "An application of the on-surface radiation condition to the scattering of acoustic waves by a reactively loaded sphere," *Wave Motion*, vol. 10, no. 3, pp. 277–284, 1988.

[14] A. Bayliss and E. Turkel, "Radiation boundary conditions for wave-like equations," *Communications on Pure and applied Mathematics*, vol. 33, no. 6, pp. 707–725, 1980.

[15] A. Bayliss, M. Gunzburger, and E. Turkel, "Boundary conditions for the numerical solution of elliptic equations in exterior regions," *SIAM Journal on Applied Mathematics*, vol. 42, no. 2, pp. 430–451, 1982.

[16] B. Engquist and A. Majda, "Absorbing boundary conditions for numerical simulation of waves," *Proceedings of the National Academy of Sciences*, vol. 74, no. 5, pp. 1765–1766, 1977.

[17] S. I. Hariharan and S. Sawyer, "Transform potential-theoretic method for acoustic radiation from structures," *Journal of Aerospace Engineering*, vol. 18, no. 1, pp. 60–67, 2005.

[18] J. G. Proakis and D. K. Manolakis, *Digital Signal Processing (4th Edition)*. Prentice-Hall, Inc., 2006.

[19] N. Berrabah, "On high order on-surface radiation boundary conditions," 2014.

[20] A. Al Weshah and S. Hariharan, "A fourier spectral method to solve high order on-surface radiation boundary conditions in electromagnetics," in *Electrical and Electronics Engineering Conference (JIEEEC), 2017 10th Jordanian International*. IEEE, 2017, pp. 1–6.

[21] D. Colton, *Partial Differential Equations: An Introduction*. Dover Publications, 2012.

[22] M. Abramowitz and I. A. Stegun, *Handbook of Mathematical Functions: With Formulas, Graphs, and Mathematical Tables*. Courier Corporation, 2012.